

**Functionalization of activated carbons by HNO<sub>3</sub> treatment: Influence  
of phosphorus surface groups**

Juan J. Ternero-Hidalgo, Juana M. Rosas, José Palomo, María J. Valero-Romero, José Rodríguez-Mirasol, Tomás Cordero \*

Universidad de Málaga, Andalucía Tech, Departamento de Ingeniería Química, Campus de Teatinos s/n, 29071 Málaga, Spain

---

\* Corresponding author:

Tel: +34 952132038. E-mail: [cordero@uma.es](mailto:cordero@uma.es) (Tomás Cordero)

**Abstract**

Influence of phosphorus on functionalization of activated carbons with nitric acid has been reviewed in this study. Results indicate that during treatment with nitric acid, phosphorus-containing carbons seem to graft more surface nitrogen, particularly as nitro groups, than those without phosphorus, where the nitrogen is found in lower oxidation state. A reaction pathway has been proposed to clarify the oxidation/nitration mechanism of phosphorus-containing carbons. The model consists of three independent mechanisms occurring simultaneously, with each one involving different phosphorus species present in the activated carbons.

Keywords: functionalization; nitric acid; phosphorus; activated carbon

## 1. Introduction

In recent decades, the use of activated carbons as adsorbents and catalysts has been steadily increasing because of their well-developed porous structure and the nature of the chemical surface, which can be modified by different treatment processes.<sup>1,2</sup> Activated carbons can be prepared from different carbonaceous precursors such as agricultural waste,<sup>3-7</sup> which possess several advantages owing to their availability, chemical composition, and low cost.

Several studies have dealt with functionalization of activated carbon to achieve the desired properties by grafting different surface groups at appropriate oxidation states. Acid or basic carbons were produced by incorporating N, O, P, S, Ca, Ba, Na or transition metals to improve their adsorption capacity or use as catalyst.<sup>8-18</sup> Oxidation resistance of activated carbons was improved by doping with P, B, or Cl,<sup>19,20</sup> whereas carbons containing N or O groups exhibited enhancement in electrochemical behaviors.<sup>21,22</sup>

Functionalization of activated carbons with nitrogen has several interesting applications. One of them is the improvement of CO<sub>2</sub> adsorption<sup>23-26</sup> and catalytic removal of NO from flue gases.<sup>27,28</sup> Other applications are related to electrochemistry: pyridinic, pyrrolic, and pyridonic nitrogen groups are electrochemically active because of the presence of more electrons.<sup>21</sup>

It is reported that the activated carbons with nitrogen have been produced by carbonizing nitrogen-containing precursors such as polyacrylonitrile<sup>29,30</sup> or surface functionalization of ammonia, urea, melamine at high temperatures, as well as via nitration reactions.<sup>27,31,32</sup>

Treatment with nitric acid is a typical method of carbon surface oxidation introducing surface oxygen-containing group.<sup>10,12,33</sup> The nitric acid treatment also introduces a small amount of surface nitrogen functional groups,<sup>27,34</sup> although most works are mainly focus on the incorporation of oxygen-surface groups, mainly as carboxyl groups. The most accepted oxidation mechanism for the treatment with nitric acid is similar to the oxidation of 9,10-dihydrophenanthrene and diphenylmethane with nitric acid,<sup>34,35</sup> where the aliphatic chains are affected, but the aromatic rings are not modified because of their high stability. Dicarboxylic and ketone groups are formed when the aliphatic chain consists of more than one (Figure 1a) and one carbon atom (Figure 1b), respectively. Mechanism of addition of a small amount of nitrogen by aromatic nitration (Figure 1c) has been described elsewhere.<sup>36</sup> This mechanism involves the formation of highly reactive nitronium ions ( $\text{NO}_2^+$ ) produced by the autoprotolysis reaction of nitric acid, similar to the self-ionization of water. In these conditions, nitronium ions appear in small quantities, because it is necessary to promote their formation by the presence of an acid catalyst such as sulfuric acid. Accordingly, some authors, more interested in introducing nitrogen in addition to oxygen, have used solutions containing nitric and sulfuric acids in different ratios, to improve the effectiveness of nitration.<sup>9,34,37,38</sup>

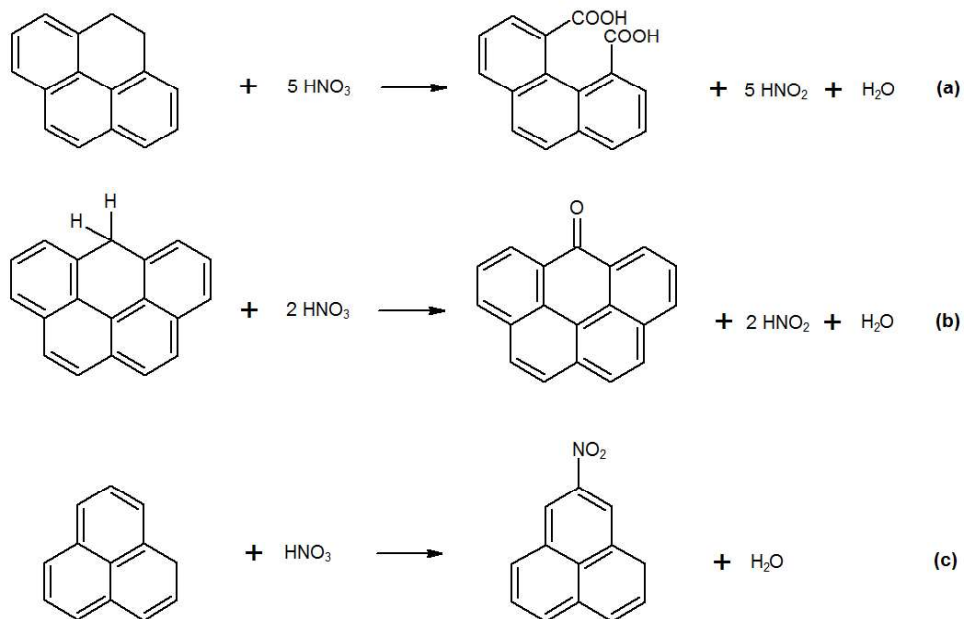


**Figure 1. Oxidation mechanisms for the treatment of activated carbons with nitric acid (adapted from refs 34,35).**

Activated carbons prepared by chemical activation using phosphoric acid contain a relatively higher amount of stable phosphorus complex, which introduces some interesting properties such as high oxidation resistance and high surface acidity.<sup>5,19</sup> In fact, such carbons have been successfully used as acid catalysts in alcohol dehydration reactions<sup>13,14</sup> and catalytic support in the selective oxidation of benzene, toluene, and xylene (BTX).<sup>15</sup> Because of the high acidity of these activated carbons, a high amount of grafted nitrogen in the form of nitro groups using only nitric acid can be expected, without a second acid reagent (e.g., sulfuric acid), as the aforementioned aromatic nitration would be catalyzed by the surface acidity of the phosphorus groups present on the activated carbon. Therefore, it would be interesting to further study the behavior of these phosphorus-containing carbons.

The purpose of this study is to investigate the influence of phosphorus on surface functionalization of different activated carbons after being treated with nitric acid.

Phosphorus-containing carbons are produced by chemical activation with phosphoric acid, and those without phosphorus are obtained by physical activation with CO<sub>2</sub>.

## **2. Experimental method**

### **2.1. Preparation of activated carbons**

Two different activated carbons were prepared by chemical and physical activation of the same precursor, olive stone supplied by Sociedad Cooperativa Andaluza Olivarera y Frutera San Isidro, Periana (Málaga), Spain. Both samples were prepared in a conventional tubular furnace at a heating rate of 10°C/min. Physically activated carbon was produced by carbonizing olive stone at 800°C for 2 h under N<sub>2</sub> flow (150 mL/min STP), followed by an activation process with CO<sub>2</sub> flow (150 mL/min STP) at the same temperature for 7 h, obtaining a burn-off of 42.5%.<sup>39,40,41</sup> This activated carbon presented a yield of 13.7% and was denoted as AC. In the case of activated carbon prepared by chemical activation, olive stone was impregnated with H<sub>3</sub>PO<sub>4</sub> 85% (w/w) at room temperature and dried for 24 h at 60°C in a vacuum dryer. The impregnation ratio (H<sub>3</sub>PO<sub>4</sub>/olive stone mass ratio) was 3:1. The impregnated substrates were activated under continuous N<sub>2</sub> flow (150 mL/min STP) at 500°C for 2 h. The activated sample was then washed with distilled water at 60°C until constant pH and vacuum-dried for 24 h at the same temperature. This activated carbon presented a yield of 44.8% and was denoted as ACP.

### **2.2. Functionalization of the activated carbons**

The activated carbons were functionalized by treatments with nitric acid or air. Functionalization with nitric acid was performed by treating 1 g of activated carbon with 50 mL of 5 M nitric acid with constant stirring at 80°C for different reaction times. Then, the samples were washed with distilled water until constant pH. The obtained

oxidized carbons were denoted by the name of the activated carbon, followed by the letter N and a number denoting the reaction time in minutes. Only N with no number represents a treatment time of 3 h. The yields after the nitric acid treatment were generally >95%.

Oxidation was performed in air by introducing 2 g of activated carbon in a tubular furnace at 350°C for 1 h under airflow (150 mL/min STP). The obtained activated carbons were denoted by the name of the activated carbon followed by the letter O. No significant weight loss was observed after the treatment with air for 2 h in ACP. By contrast, the same treatment carried out to AC resulted in a yield <75%.

Other activated carbons, from ACP, were prepared by treatments with air and nitric acid in different sequences. The reaction conditions were similar as before, in this case, the reaction time of the nitric acid treatment being 3 h. The nomenclature used was the name of the activated carbon followed by the letters N or O considering the chronological order of the treatments. For instance, ACP-NON is a carbon that has been treated with nitric acid (3 h), followed by air (1 h), and finally with nitric acid (3 h). In all cases, the yields obtained after the nitric acid and air oxidation treatments were >95%.

### 2.3. Characterization of samples

The porous structure of the samples was characterized by N<sub>2</sub> adsorption–desorption and CO<sub>2</sub> adsorption at –196 and 0°C, respectively, using a micromeritics instrument (ASAP 2020 model). The samples were previously outgassed for at least 8 h at 150°C. From the N<sub>2</sub> isotherm, the apparent surface area ( $A_{\text{BET}}$ ) was determined by applying the BET equation; micropore volume ( $V_t$ ) and external surface area ( $A_t$ ) were calculated using the t-method; and mesopore volume ( $V_{\text{mes}}$ ) was determined as the difference between

the maximum adsorbed volume of  $N_2$  ( $V_p$ ) and the micropore volume ( $V_t$ ). From the  $CO_2$  adsorption data, the narrow micropore volume ( $V_{DR}$ ) and surface area ( $A_{DR}$ ) were calculated using the Dubinin–Radushkevich equation.

Surface chemistry of the samples was analyzed by X-ray photoelectron spectroscopy (XPS) and temperature-programmed desorption (TPD). XPS analyses of the samples were obtained by a 5700C model Physical Electronics apparatus with  $MgK\alpha$  radiation (1253.6 eV). The maximum of the C1s peak was set at 284.5 eV and used as a reference to shift the other peaks.<sup>13</sup> The peaks were deconvoluted by least squares using Gaussian–Lorentzian peak shapes and a Shirley-type background line.

TPD profiles were obtained in a custom quartz fixed-bed reactor placed inside an electrical furnace. The samples were heated from room temperature to 930°C at a heating rate of 10°C/min in  $N_2$  flow (200 cm<sup>3</sup> STP/min). The amounts of CO and  $CO_2$  desorbed from the samples were monitored by nondispersive infrared (NDIR) gas analyzers (Siemens ULTRAMAT 22).

Elemental analysis of the samples was performed using a PerkinElmer 2400 CHN system, and the oxygen content was calculated by difference. The ash contents of the samples were obtained from the weight of the solid residue after exposure to air-TG at 900°C.

The surface texture and structure of the samples were characterized by scanning electron microscopy (SEM). Scanning electron micrographs were obtained at a high voltage of 20–25 kV, using a JEOL JSM-840 instrument equipped with energy-dispersive X-ray analysis (EDXA).

The possible presence of phosphorus in the aqueous solution was analyzed by a colorimetric technique based on the formation of a blue phosphorus complex, following

the testing procedure described elsewhere.<sup>42</sup> This technique involves the reaction of ammonium molybdate and potassium antimony tartrate with orthophosphate in an acid medium to form an antimony–phospho–molybdate complex. The reduction of this complex by ascorbic acid produces an intense blue solution. Only phosphorus as orthophosphate can react with the molybdate reagent. In this case, it is considered that probably all the phosphorus in solution be of this form, because of the fact that surface phosphorus complexes are possibly oxidized during the high exposure of activated carbon with nitric acid at 80°C during nitration. Arsenic as arsenate in the solution might cause a positive interference, as it can also react with the molybdate reagent to produce a blue solution; however, this possible effect was considered negligible, because the carbons were free of arsenic compounds. In order to perform the analysis, first, the samples in nitric acid medium were filtered and neutralized using phenolphthalein indicator and 1M NaOH solution. Then, 10 mL of previously diluted neutralized solution and 8 mL of molybdate colorimetric solution were mixed thoroughly for 10 min at room temperature. The molybdate colorimetric solution was prepared in accordance with the description of Pote and Daniel.<sup>42</sup> Finally, the absorbance of each sample was measured at 850 nm in a Varian Cary 50 Conc UV–Vis Spectrophotometer using a sample blank (nitric acid and molybdate colorimetric solution) as the reference solution.

### **3. Results and discussion**

#### **3.1. Influence of phosphorus**

##### **3.1.1. Porous structure**

Figure 2 shows the N<sub>2</sub> adsorption–desorption isotherms at –196°C for the different activated carbons prepared, while Table 1 summarizes the values of the structural parameters that characterize the porous structure calculated from N<sub>2</sub> adsorption–

desorption and CO<sub>2</sub> adsorption isotherms of the samples, including the treatments with nitric acid at different reaction times. On the one hand, ACP presents a type IV isotherm, corresponding to a well-developed micro- and mesoporous structure, as a large amount of N<sub>2</sub> is adsorbed in the entire relative pressure range. On the other hand, AC shows a type I isotherm indicating that it is essentially microporous, as all the N<sub>2</sub> is adsorbed at low relative pressures. H4-type hysteresis loops are observed for all the activated carbons often associated to slit-shaped pores.

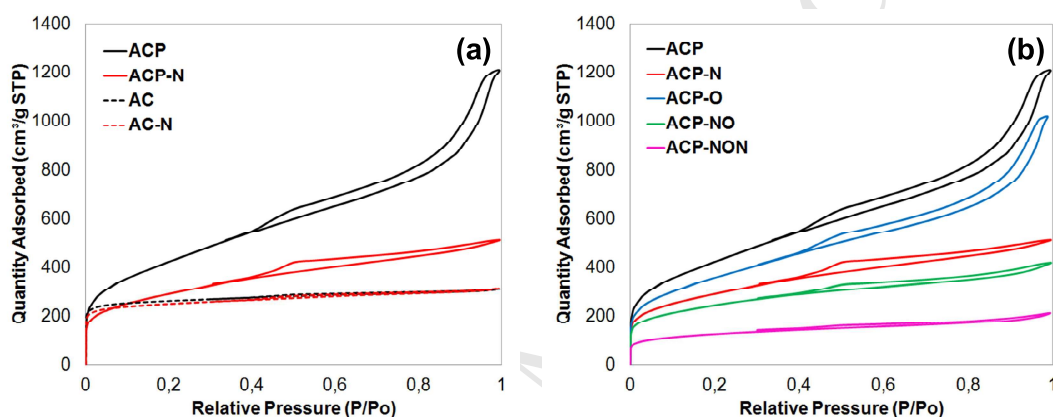


**Figure 2.** N<sub>2</sub> adsorption–desorption isotherms at  $-196^{\circ}\text{C}$  of the activated carbons. (a) Before and after treatment with nitric acid for 3 h; (b) before and after different treatments with nitric acid for 3 h and air.

The sample ACP shows high external surface area ( $A_t$ ) and mesopore volume ( $V_{\text{mes}}$ ). A small difference between  $V_p$  and  $V_{\text{mes}}$  reveals the significant contribution of mesoporosity. The activated carbon prepared by physical activation exhibits a significantly narrower microporosity than the one prepared by chemical activation, which is evidenced by the much closer  $A_{\text{BET}}$  and  $A_{\text{DR}}$  values.

**Table 1. Porous structural parameters calculated from N<sub>2</sub> adsorption–desorption and CO<sub>2</sub> adsorption of the activated carbons before and after the different treatments of functionalization.**

Sample	N <sub>2</sub> isotherm					CO <sub>2</sub> isotherm	
	A <sub>BET</sub> (m <sup>2</sup> /g)	V <sub>p</sub> (cm <sup>3</sup> /g)	V <sub>mes</sub> (cm <sup>3</sup> /g)	A <sub>t</sub> (m <sup>2</sup> /g)	V <sub>t</sub> (m <sup>2</sup> /g)	A <sub>DR</sub> (m <sup>2</sup> /g)	V <sub>DR</sub> (cm <sup>3</sup> /g)
AC	922	0.48	0.11	106	0.37	864	0.35
AC-N	902	0.48	0.14	119	0.35	1028	0.36
ACP	1532	1.86	1.45	796	0.42	600	0.24
ACP-N5	1286	1.46	1.16	708	0.30	540	0.22
ACP-N20	1250	1.37	1.07	667	0.30	548	0.22
ACP-N	1045	0.79	0.46	406	0.32	542	0.22
ACP-O	1288	1.57	1.25	707	0.32	497	0.20
ACP-ON	877	0.66	0.37	303	0.29	410	0.16
ACP-NO	874	0.65	0.34	248	0.31	485	0.20
ACP-NON	442	0.33	0.18	119	0.15	335	0.13

The results show that the oxidation/nitration of the activated carbons with nitric acid and/or air results in a decrease of porosity, although this effect is more pronounced in the case of nitric acid treatment. As can be seen, nitric acid treatment can substantially modify the porous structure of the activated carbon. However, the mechanism of modifying the porous structure is not well established, and different hypothesis can be found in the literature.<sup>11,33,34,43,44</sup> It is noteworthy that, in general, the activated carbons used in those studies are essentially microporous and present a less-developed porous structure than the samples used in this study. In any case, most of the authors observed a decrease of micropore volume and surface area. In addition to this effect, some authors observed an increase of mesopore volume. In general, it has been proposed in the literature that nitric acid can act in two different ways, blocking the micropores or destroying/degrading the porous structure. The pore blockage is usually related to the fixation of oxygen groups at the entrance and/or on the walls of micropores<sup>11</sup>; however, in some studies, it has also been described to be associated with the formation of humic substances during the oxidation process.<sup>34</sup>

The results shown in Figure 2 suggest that nitric acid acts differently on the porous structure, depending upon the activated carbon used. In the case of AC, it only produces small changes on the porous structure,<sup>11,33,34,43,44</sup> a slight decrease of  $V_t$  and  $A_t$ , and a small increase of  $V_{mes}$ . However, the effect of nitric acid in ACP is more pronounced, particularly affecting the mesopores and decreasing  $V_{mes}$  (from 1.45 to 0.46 cm<sup>3</sup>/g) and  $A_t$  (from 796 to 406 m<sup>2</sup>/g) after 3 h of reaction. This substantial decrease of the porosity is much higher than those reported in the aforementioned studies. This decrease of  $V_{mes}$  and  $A_t$  could be attributed to partial gasification of the carbon particles. In addition, a decrease in the particle size has been observed. Similar results have been reported in a previous study on the oxidation of phosphorus-containing activated carbons in the presence of air.<sup>19</sup> If porous blockage occurred, a thermal treatment was performed after the nitric acid treatment for clarity. The results (not shown) indicated no recovery of porosity after desorption of the created surface groups.

It can also be observed from Table 1 that ACP-NO and ACP-ON present similar structural parameters, suggesting that the order of the treatments with air and nitric acid does not affect the final porous structure of the activated carbons. It is interesting to note that the nitric acid treatment practically reduced the value of  $V_p$  by half, even after air oxidation. In this context, the most oxidized carbon (ACP-NON) presents the lowest structural parameter values.

### 3.1.2. Surface chemistry

Results of the elemental analysis and the mass surface concentrations determined by XPS of the samples are reported in Table 2. It can be observed that the main elements found on the fresh activated carbon surfaces were carbon and oxygen, with a small amount of phosphorus on the one prepared by chemical activation using H<sub>3</sub>PO<sub>4</sub>, because

of the presence of surface phosphorus complexes formed during the activation step, which seem to be stably bonded to carbon as they do not elute after washing with distilled water.<sup>4,5</sup>

After treatment with nitric acid, the amount of oxygen and nitrogen increased,<sup>10,12,23,33,34</sup> but this increase is more pronounced in ACP than AC. These differences seem to be initially related to the presence of phosphorus. A comparison between the increases of surface nitrogen content determined by XPS (from the outer surface) and elemental analysis (from the bulk) of ACP treated with nitric acid suggests that the reaction takes place uniformly throughout the particle. This is evidenced by the fact that the increases obtained by both techniques are quite similar. However, in the case of AC, the reaction with nitric acid seems to be more important on the outermost surface than inside, as the amount of nitrogen analyzed in AC-N is higher in XPS than elemental analysis.

**Table 2. Elemental analysis and mass surface concentration (%) determined by XPS of the activated carbons.**

Sample	XPS (wt%)				Elemental Analysis (wt% d.a.f.)			
	C1s	O1s	N1s	P2p	C	H	N	O*
AC	93.5	6.3	0.2	0	84.1	0.6	0.3	15.0
AC-N	82.1	16.1	1.8	0	70.9	2.3	1.1	25.8
ACP	90.8	6.6	0.3	2.2	85.9	2.8	0.1	11.2
ACP-N5	81.8	14.7	1.9	1.7	79.3	2.5	1.7	16.5
ACP-N20	79.7	17.3	2.2	0.8	72.7	3.0	2.1	22.2
ACP-N	76.4	20.4	2.3	0.9	62.8	3.3	2.0	31.9
ACP-O	83.4	14.3	0.4	2.0	75.7	2.2	0.4	21.7
ACP-ON	77.5	20.3	1.6	0.6	63.1	2.3	1.6	32.9
ACP-NO	78.6	19.2	1.4	0.8	62.1	2.0	1.2	34.7
ACP-NON	65.1	32.4	2.0	0.5	57.6	2.3	1.8	38.2

\* by difference; d.a.f: dry ash-free basis

SEM micrograph and the corresponding EDXA elemental mappings of ACP-N are depicted in Figure 3. It is interesting to note that the distribution of the different

heteroatoms present in the carbon ACP-N (phosphorus, oxygen, and nitrogen) is quite uniform. This indicates that the treatments carried out in this study act uniformly on the entire surface. As mentioned earlier, phosphorus results from the activation process, while most of the oxygen and nitrogen atoms result from the nitric acid treatment.

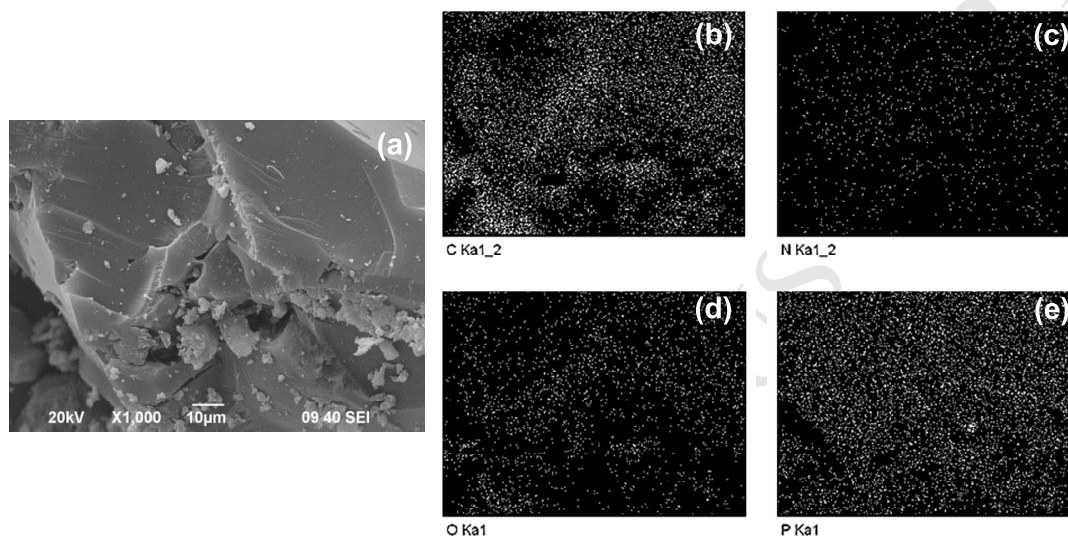


**Figure 3.** SEM micrograph (a) and EDXA C (b), N (c), O (d), and P (e) elemental mappings of ACP-N.

The N1s XPS spectra of the activated carbons (before and after treatment with nitric acid) have been studied (Figure 4) to identify the chemical state of N groups. It can be observed that the nature of the introduced surface nitrogen is very different in both activated carbons, ACP-N and AC-N. The N1s spectrum of ACP-N presents mainly a peak centered at 405.7 eV corresponding to nitro groups. Nevertheless, AC-N presents two peaks, the first one corresponding to nitro groups and the second one at lower binding energies attributed to more reduced nitrogen such as nitroso (N-O at 400.1 eV), pyrrolic (C-N(5) at 400.4 eV), and pyridinic (C-N(6) at 398.9 eV) groups.<sup>30</sup> Therefore, not only ACP incorporates higher amounts of nitrogen, but also this nitrogen is selectively found as nitro groups. These results suggest that phosphorus could be involved in the oxidation/nitration mechanism, playing an important role in the

functionalization of the activated carbon. Consequently, a different surface chemistry is obtained after treatment with nitric acid on phosphorus-containing carbons.

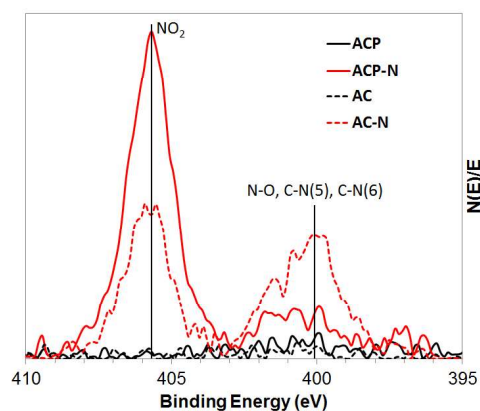


Figure 4. N1s XPS spectra of ACP and AC before and after nitric acid treatment for 3 h.

### 3.2. Influence of reaction time

In order to perform an in-depth analysis of the oxidation/nitration mechanism in phosphorus-containing carbons, different treatments with nitric acid have been carried out to ACP at different reaction times (5, 10, 15, 20, 60, and 180 min), but only 5, 20, and 180 min have been reported to gain a clear understanding. Regarding the porous structure, it can be observed in Table 1 that the degradation produced by nitric acid is more pronounced with the increase of reaction time.

The evolution of surface chemistry during the reaction was analyzed by XPS and TPD. XPS technique has been particularly used to evaluate the possible changes occurred with respect to nitrogen and phosphorus during the nitric acid treatment. It is observed in Table 2 that longer reaction times result in higher oxygen and nitrogen surface concentrations, as well as lower phosphorus surface concentration. The changes in the surface concentration of nitrogen and phosphorus are mainly produced during the first 20 min, and no significant changes are observed after 3 h. The N1s and P2p XPS

spectra of the ACP at different reaction times are presented in Figure 5. The selective formation of nitro groups can be observed in the N1s spectra (Figure 5a), in which a main peak at 405.7 eV is detected. Furthermore, the figure also shows an increase in the levels of these groups (peak) during the progress of the reaction. It is noteworthy that the P2p spectrum of ACP is also affected after treatment with nitric acid. At the beginning, mainly three different P2p peaks were found in the XPS spectrum of ACP, corresponding to surface phosphorus groups such as C<sub>3</sub>-PO (132 eV), C-PO<sub>3</sub>/C<sub>2</sub>-PO<sub>2</sub> (133.1 eV), and C-O-PO<sub>3</sub>/(C-O)<sub>3</sub>PO (134 eV).<sup>13</sup> In the previous studies, the possible presence of C<sub>3</sub>-P-type groups at 131 eV was investigated, and it was found that the formation of this complex is negligible during the chemical activation process with phosphoric acid<sup>19</sup>; therefore, the presence of C<sub>3</sub>-P-type groups has not been considered in this study. On the contrary, the P2p spectrum intensity diminishes during the reaction and the maximum value shifts to lower binding energies, moving into the region of C-PO<sub>3</sub>/C<sub>2</sub>-PO<sub>2</sub> groups. These results indicate that the amount of C-O-PO<sub>3</sub>-type groups is reduced and the C<sub>3</sub>-PO-type groups are oxidized in favor of C-PO<sub>3</sub>/C<sub>2</sub>-PO<sub>2</sub>-type groups. A possible explanation for the reduction of phosphorus content in the form of C-O-PO<sub>3</sub> groups could be the formation from these groups of phosphoric acid, which would remain in the aqueous solution.

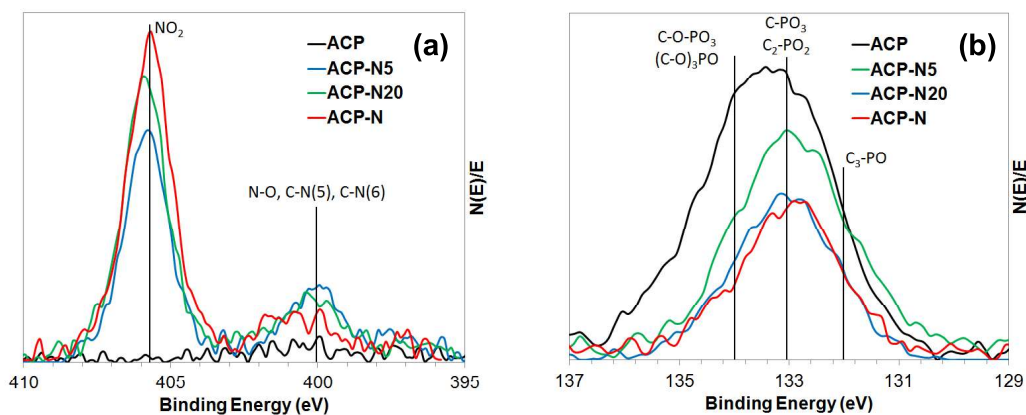


Figure 5. N1s (a) and P2p (b) XPS spectra of ACP after nitric acid treatment at different times.

TPD is a technique used to characterize in detail the carbon–oxygen groups of the samples. The acidic groups (carboxyl, and lactonic) evolve as  $\text{CO}_2$ , whereas the nonacidic (carbonyl, ether, and quinone) and phenol groups decompose as  $\text{CO}$ . Anhydride surface groups evolve as both  $\text{CO}$  and  $\text{CO}_2$ .<sup>2</sup>

Figure 6 shows the evolution of  $\text{CO}_2$  and  $\text{CO}$  from TPD analysis of ACP at different reaction times with nitric acid. It is evident from the figure that ACP presents a higher  $\text{CO}$  evolution than  $\text{CO}_2$ . Most of  $\text{CO}$  is desorbed at high temperatures ( $800^\circ\text{C}$ ), which can be attributed to the presence of  $\text{C-O-PO}_3$  groups formed during the activation of phosphoric acid, as reported by Wu and Radovic<sup>20</sup> and our previous studies.<sup>5,19</sup> A small amount of  $\text{CO}$  is desorbed at temperatures below  $800^\circ\text{C}$ , because of the presence of anhydride ( $600^\circ\text{C}$ ), phenol ( $650^\circ\text{C}$ ), and ether ( $700^\circ\text{C}$ ) groups. The amount of  $\text{CO}_2$  evolved is significantly lower than  $\text{CO}$ , indicating a lower concentration of carboxyl ( $300^\circ\text{C}$ ), lactonic ( $400^\circ\text{C}$ ), and anhydride ( $600^\circ\text{C}$ ) groups.

An increase in the amount of  $\text{CO}$  and  $\text{CO}_2$  desorption observed after treatment with nitric acid is attributed to the strong oxidation. The intensity of this oxidation is observed to be more at higher reaction times because of the progressive formation of carboxyl, lactonic, anhydride, and particularly phenol groups (Figure 6). It is interesting

to note that the CO evolution for these activated carbons remains constant after 20 min of reaction, where a decrease in the contribution of CO evolved at 800°C (attributed to C-O-PO<sub>3</sub> groups) with respect to the initial carbon was observed. This indicates the possible removal of C-O-PO<sub>3</sub> groups during the oxidation with nitric acid.

TPD of both AC and AC-N was performed. The treatment with nitric acid produces carbon-oxygen groups similar to ACP-N, but the amount of these groups is much higher in the latter.

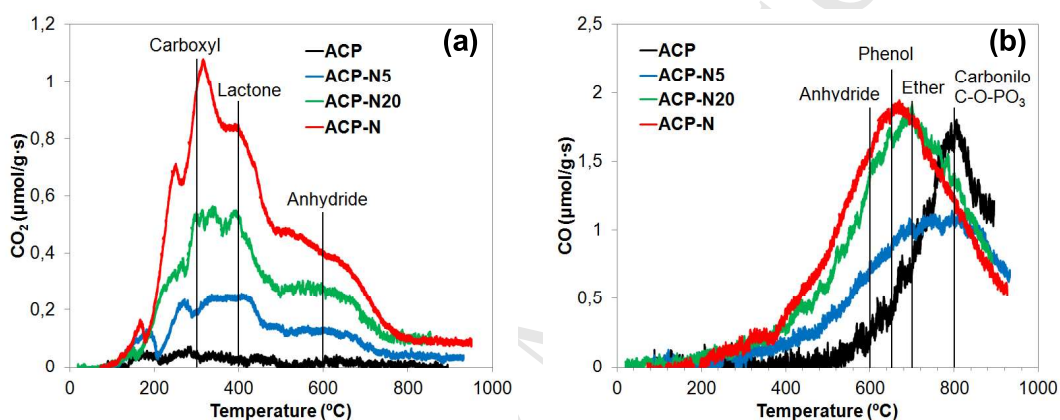


Figure 6. CO<sub>2</sub> (a) and CO (b) evolution during the TPD of ACP after nitric acid treatment at different reaction times.

### 3.3. Oxidation/nitration mechanisms

On the basis of the results of XPS and TPD, three different oxidation/nitration mechanisms have been proposed to explain the effect of nitric acid treatment on phosphorus-containing carbons, changes of surface groups, and selective production of large amount of nitro groups on ACP samples after the treatment. These mechanisms would take place simultaneously with each involving one of the different phosphorus species: C<sub>3</sub>-PO-, C-PO<sub>3</sub>/C<sub>2</sub>-PO<sub>2</sub>-, or C-O-PO<sub>3</sub>/(C-O)<sub>3</sub>PO-type groups. In these groups, the P atoms can be bonded directly to carbon surface in the form of C-P, as well as to a carbon through an O atom in the form of C-O-P. With regard to the changes of

phosphorus groups, the results showed that the C-O-PO<sub>3</sub> groups of ACP are removed after the reaction with nitric acid, as can be observed by the lower CO evolution at 800°C from TPD (Figure 6b) and lower contribution of C-O-PO<sub>3</sub> in the P2p XPS spectra (Figure 5b). These results could support the potential energy surface scan calculations carried out by Wu and Radovic,<sup>20</sup> which showed the higher dissociation energy of C-P bonds than the C-O and O-P bonds belonging to C-O-P system.

According to the P2p XPS results (Figure 5b), the phosphorus complexes containing C-P bonds are not removed after the nitric acid treatment, with C-PO<sub>3</sub> contributing to the majority of phosphorus surface group. This indicates that parts of the C<sub>3</sub>-PO groups are oxidized to C<sub>2</sub>-PO<sub>2</sub> and C-PO<sub>3</sub> groups during the reaction. At the same time, a large amount of nitro groups are formed during the above oxidation reactions of phosphorus.

All the proposed mechanisms assume that, during the nitric acid treatment, the phosphorus complexes are responsible for the formation of nitronium ions, which are capable of performing aromatic nitration. In this way, the nitro groups would be present near the phosphorus species, which is supported by the results obtained in the EDXA elemental mappings shown in Figure 3, where a uniform distribution of the nitrogen and phosphorus atoms is observed.

### 3.3.1. Nitration mechanism involving C-PO<sub>3</sub> groups

As previously mentioned, the aromatic nitration with nitric acid is enhanced in the presence of an acid catalyst. The acid character of these phosphorus-containing activated carbons, which renders them interesting catalytic properties, has been already reported in our previous works. In fact, they have been successfully used as acid catalysts in alcohol dehydration reactions.<sup>13-14</sup> Accordingly, the proposed mechanism

suggests the formation of nitro groups on the carbon surface, while the phosphorus groups act as an acid site, promoting the catalysis of the aromatic nitration.

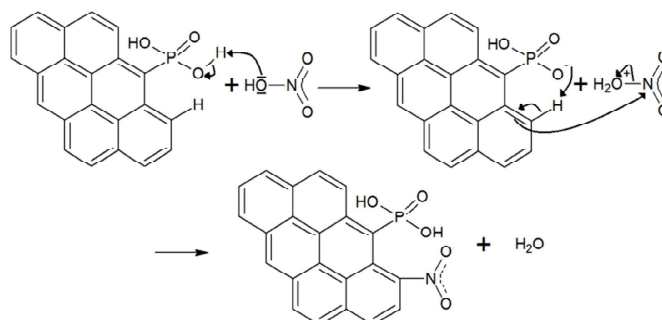


**Figure 7. Oxidation mechanism with C-PO<sub>3</sub> groups during nitric acid treatment.**

The highly reactive nitronium ion (NO<sub>2</sub><sup>+</sup>) is generated after the protonation of nitric acid (Figure 7), being the active species of the aromatic nitration via electrophilic aromatic substitution. In this case, the nitration is highly favored. In fact, a large amount of nitro groups is grafted on the carbon surface, because the protonation takes place near the aromatic structure, which is very important as the nitronium ion is not very stable and it must carry out the nitration quickly before disappearing.<sup>36</sup>

### 3.3.2. Nitration mechanism involving C<sub>3</sub>-PO groups

This mechanism involves phosphorus complexes with lower oxidation states. The XPS results showed the shift of P2p spectrum to the region of C-PO<sub>3</sub>/C<sub>2</sub>-PO<sub>2</sub> groups. Therefore, the formation of nitro groups must be associated with the oxidation of the C<sub>3</sub>-PO into C-PO<sub>3</sub>/C<sub>2</sub>-PO<sub>2</sub> groups.

It can be observed from the scheme proposed in Figure 8 that the P=O bond is protonated followed by a nucleophilic attack by the nitrate anion. This step may be due to the polarization of the P=O bond, as the oxygen atom is more electronegative than the phosphorus atom. This mechanism does not take place in C-PO<sub>3</sub> groups, because the

polarization of the P=O bond is less pronounced as the phosphorus atom is bonded to two oxygen atoms more. Therefore, the nucleophilic attack is not favored.

Then, the nitrate bonded to the phosphorus atom is protonated producing a nitronium ion (Figure 8), which can carry out the aromatic nitration. At the same time, the P=O bond is recovered releasing a proton.

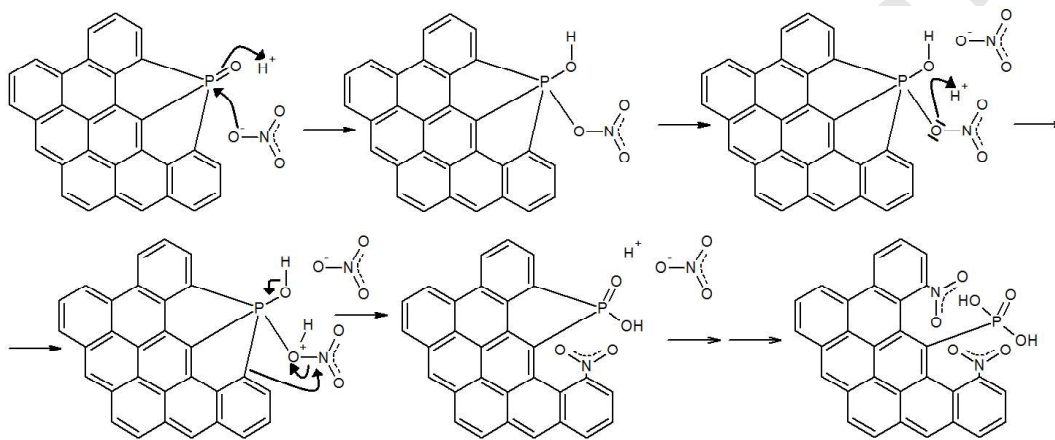


Figure 8. Oxidation mechanism with C<sub>3</sub>-PO groups during nitric acid treatment.

### 3.3.3. Nitration mechanism involving C-O-PO<sub>3</sub> groups

It is noteworthy that the phosphorus complexes formed after the chemical activation with phosphoric acid are very stable. In fact, they are not removed after washing with distilled water. However, the results of XPS analyses suggest that the C-O-PO<sub>3</sub>/(C-O)<sub>3</sub>-PO<sub>3</sub>-type groups are susceptible of being removed probably as phosphoric acid after treatment with nitric acid, resulting in the formation of surface phenol (Figure 6b) and nitro groups (Figure 9). As explained earlier, the C-O and O-P bonds belonging to C-O-P system have lower dissociation energy than the C-P bonds in the phosphorus groups; this may explain the removal of phosphorus as phosphoric acid.

In this way, the other proposed mechanism is depicted in Figure 9. First, the oxygen of the P=O bond is protonated, and simultaneously, a nitrate anion is bonded to the C-O-P

system. Then, the O-P bond is broken and a phenol group is formed. At the same time, phosphoric acid in solution is released and a nitro group is formed.

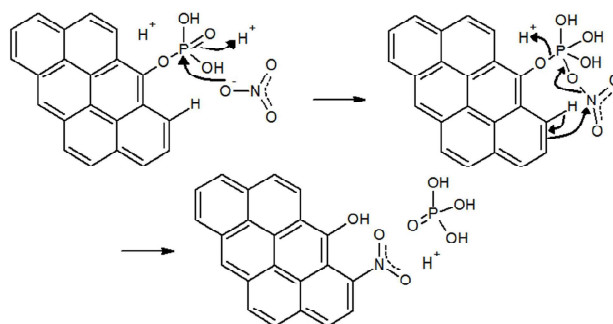


**Figure 9. Mechanism on C-O-PO<sub>3</sub> groups during nitric acid treatment.**

As can be derived, this mechanism is the least productive for the formation of nitro groups among all the proposed mechanisms, because part of phosphorus is removed.

In order to check whether the proposed mechanisms are valid, additional experiments were performed. These experiments consist of alternating treatments with air and nitric acid on the same activated carbon.

### 3.4. Air–nitric acid treatment

Wu and Radovic<sup>20</sup> proposed that carbons doped with phosphorus groups present high oxidation resistance. It was reported in our previous results that the phosphorus complexes formed on the carbon during the chemical activation with phosphoric acid are responsible for the improvement of the oxidation resistance. The mechanism involves the oxidation of C<sub>3</sub>-PO, C<sub>2</sub>-PO<sub>2</sub>, and C-PO<sub>3</sub> surface groups into C-O-PO<sub>3</sub>, (CO)<sub>2</sub>-PO<sub>2</sub>, and (CO)<sub>3</sub>-PO as the first step (Figure 10), delaying the gasification reaction of the carbonaceous matrix.<sup>19</sup> In this study, a thermal treatment under airflow at 350°C was carried out to ensure that most of phosphorus groups were in the form of C-O-PO<sub>3</sub> groups. According to the above-described mechanism, a subsequent treatment with nitric acid should remove more phosphorus groups in ACP-ON with respect to ACP-N,

and consequently, a lower amount of nitro groups and more formation of phenol groups would be expected in ACP-ON.

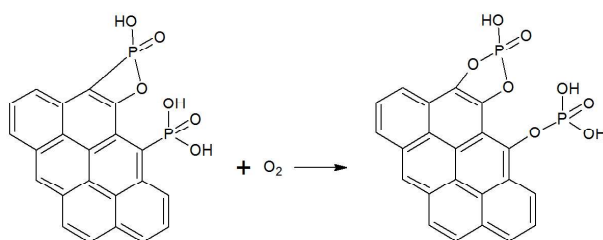
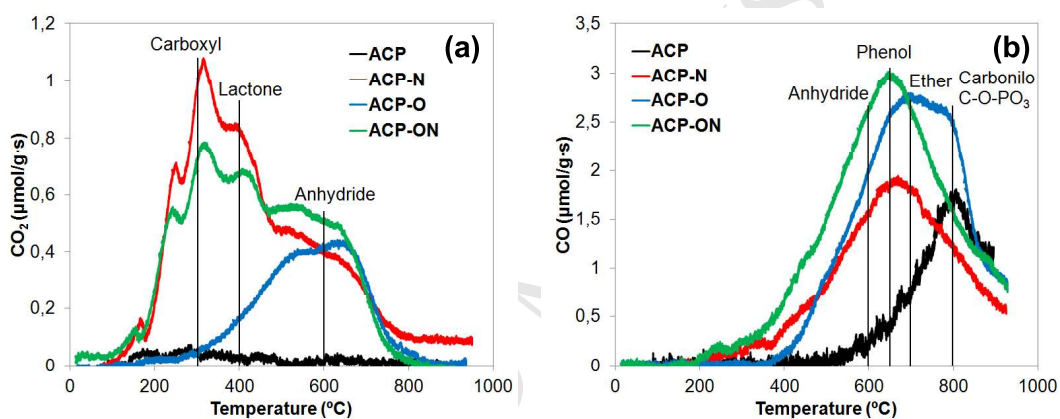


**Figure 10. Oxidation of phosphorus groups bonded to the carbon after a thermal treatment under airflow.**

In this context, determination of phosphorus in solution by a colorimetric technique was carried out in the resulting solutions after the treatments on ACP and ACP-O to corroborate if the phosphorus bound to the carbon can be hydrolyzed to the orthophosphate form in solution after the nitric acid treatment. Both samples showed a blue appearance after the addition of the molybdate colorimetric solution, which indicated the positive presence of phosphorus in solution. These results confirm that the phosphorus groups present on the activated carbon can be removed by the action of nitric acid. Besides, as predicted by the proposed mechanisms, this removal was more pronounced in the carbon previously treated with air.

Figure 11 shows the evolution of CO<sub>2</sub> and CO from TPD analysis of ACP, ACP-N, ACP-O, and ACP-ON. It can be observed that the CO<sub>2</sub> evolutions of ACP-N and ACP-O are different. In particular, the nitric acid treatment increased the concentration of carboxyl groups, as well as lactonic and anhydride groups.<sup>43</sup> However, carboxyl groups are not formed during the oxidation with air as a result of the temperature used in the air treatment (350°C). Consequently, it only increased the CO<sub>2</sub> evolution at high temperature, which is attributed to the presence of lactonic and anhydride groups.

Similar results were previously reported.<sup>2</sup> The air treatment induced an increase of the CO evolution in ACP-O at 800°C, indicating the formation of C-O-P bonds, as expected (Figure 10). After the treatment with nitric acid, the CO evolution in ACP-ON shifts to lower temperatures, indicating a decrease of C-O-P bonds and increase of phenol groups (650°C) according to the proposed mechanism with C-O-PO<sub>3</sub> groups (Figure 9). Moreover, it is interesting to note that the CO evolution at 650°C (attributed to phenol groups) is higher in ACP-ON than in ACP-N, because of the higher amount of C-O-PO<sub>3</sub> groups in ACP-O than in ACP, starting carbons in both cases.



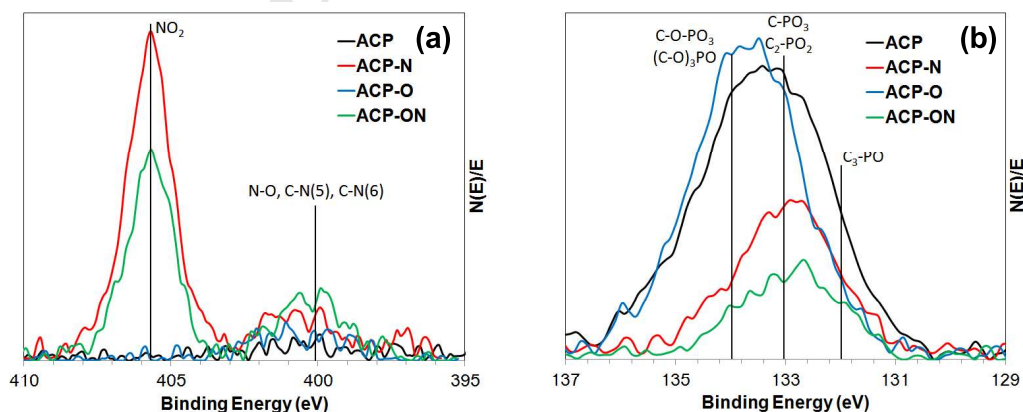
**Figure 11.** CO<sub>2</sub> (a) and CO (b) evolution during the TPD of the activated carbons after nitric acid and/or air treatments.

Table 2 also shows that after the treatment with nitric acid, the phosphorus surface concentration is lower on ACP-ON than on ACP-N. Besides, the amount of grafted nitrogen is lesser on ACP-ON than on ACP-N. These results support the proposed mechanism on C-O-PO<sub>3</sub> groups, which predicts a lower amount of grafted nitrogen and larger quantity of phosphorus removed during the HNO<sub>3</sub> treatment on ACP-O than on ACP.

The N1s and P2p XPS spectra of the ACP after nitric acid and/or air treatment are depicted in Figure 12. The N1s spectrum confirms that the grafted nitrogen atoms on

ACP-ON are preferentially nitro groups. With regard to the P2p spectra, it can be observed that the maximum value shifts to higher binding energies in ACP-O, moving into the region of C-O-PO<sub>3</sub>/(C-O)<sub>3</sub>-PO<sub>3</sub> groups. Furthermore, the P2p spectrum shifts to lower binding energies in ACP-ON, which is attributed to C-PO<sub>3</sub>/C<sub>2</sub>-PO<sub>2</sub> groups, and the intensity diminishes even below that of ACP-N, as a consequence of a decrease in phosphorus content.

On the basis of the proposed mechanisms, it may be possible to estimate the nitrogen gain (as -NO<sub>2</sub> groups) after treatment with nitric acid, if the amount of phosphorus removed is known. In this context, the carbon sample ACP-ON is used for investigation, because it is derived from ACP-O, which has few types of phosphorus, mainly as C-O-PO<sub>3</sub>/(C-O)<sub>3</sub>-PO<sub>3</sub> and C-PO<sub>3</sub>/C<sub>2</sub>-PO<sub>2</sub> groups. The atomic concentrations obtained by XPS are used for calculations, which can be deduced from Table 2. It is suggested that for each phosphorus atom removed, a nitro group is formed, and for each remaining phosphorus atom (in a reduced state), two nitro groups are formed. Then, the atomic surface concentration of nitrogen is calculated to be 1.3% versus the real value of 1.5%. These results also support the mechanisms proposed in this study.



**Figure 12.** N1s (a) and P2p (b) XPS spectra of the activated carbons after nitric acid and/or air treatments.

### 3.5. Nitric acid–air–nitric acid treatment

Finally, the carbon ACP-NON was prepared to check whether the remaining phosphorus in ACP-N can be oxidized with air and then removed with nitric acid, obtaining nitro groups.

The N1s and P2p XPS spectra are presented in Figure 13. It can be observed from the P2p spectrum of ACP-NO that the treatment of ACP-N with air continues forming C-O-PO<sub>3</sub>-type groups. Moreover, when ACP-NO is treated with nitric acid, a higher amount of phosphorus is removed and more nitro groups are formed (Figure 13b), supporting the proposed mechanism on C-O-PO<sub>3</sub> groups. Table 2 shows that the treatment of ACP-N with air produces a decrease in oxygen and nitrogen atoms because of the elimination of the less-stable thermal oxygen and nitrogen functional groups (carboxyl and nitro groups), which is attributed to the temperature of 350°C. The remaining nitrogen is in a reduced state in the N1s spectrum, as opposite to the nitro group.

It is interesting to note the high oxygen surface concentration of 26.7% on ACP-NON. This indicates that the air treatment generates new active sites (e.g., by dearomatization), where a stronger oxidation is produced by nitric acid attack. It is likely that the treatment with air dearomatizes the graphitic structure, rendering the aliphatic chains susceptible for oxidation.<sup>34,35</sup>

The above-described calculations to estimate the grafted nitrogen have also been carried out in ACP-NON considering that ACP-NO initially presented a nitrogen surface concentration of 1.3%. The atomic surface concentration of nitrogen is calculated to be 1.9% (1.3% of initial nitrogen and 0.6% of nitro groups formed) versus the real value of 1.8%. These results also seem to corroborate the proposed model.

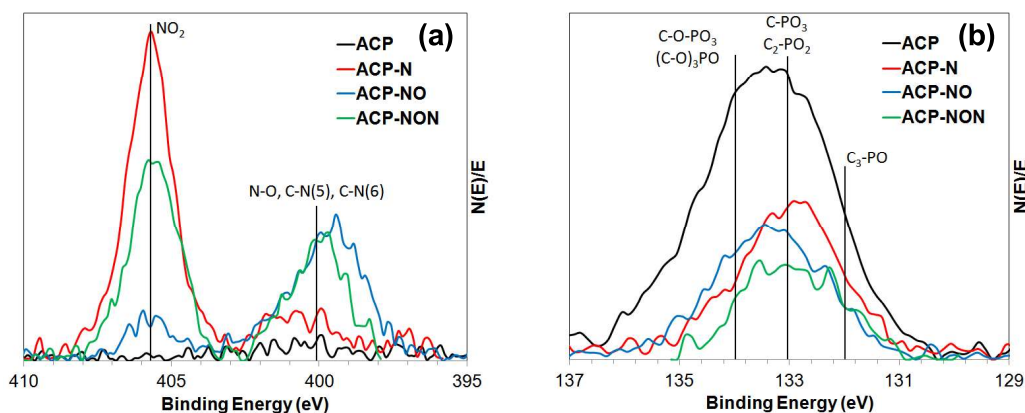


**Figure 13. N1s (a) and P2p (b) XPS spectra of the activated carbons after nitric acid and/or air treatments.**

#### 4. Conclusions

Activated carbons prepared by chemical activation with  $\text{H}_3\text{PO}_4$  can form a relatively larger amount of N surface functional groups by  $\text{HNO}_3$  treatment than carbons prepared by  $\text{CO}_2$  physical activation. The presence of phosphorus species is probably responsible for such a difference. In P-containing carbons, the formed N groups are mainly in the form of nitro groups, while the N species are mainly in the form of lower oxidation states in P-free carbons.

Three possible reaction mechanisms involving different P species are proposed to explain the nitration processes occurred during  $\text{HNO}_3$  treatment of P-containing carbons. First, the presence of  $\text{C-PO}_3$  groups on carbon surface may act as acid sites for the protonation of nitric acid, which forms nitronium ion. This highly reactive ion is the active species in the aromatic nitration via electrophilic aromatic substitution. Second, the P species at lower oxidation states such as  $\text{C}_3\text{-PO}$  may be oxidized to  $\text{C}_2\text{-PO}_2/\text{C-PO}_3$  groups during  $\text{HNO}_3$  treatment, and the protonation of the nitrate bonded to the P atom forms a nitronium ion, which results in the formation of nitro groups ( $-\text{NO}_2$ ) on carbon surface. Third, the  $\text{C-O-PO}_3/(\text{C-O})_3\text{PO}$  groups are detached from carbon surface when

they react with  $\text{HNO}_3$  to form phosphoric acid (in the solution), phenol, and nitro surface groups. These three mechanisms may take place simultaneously and most likely are responsible for the formation of nitro surface groups in P-containing carbons.

### Acknowledgments

This study was supported by the Spanish Ministry of Economy and Competitiveness under CTQ2012-36408 project and Junta de Andalucía (P09-FQM-5156 and P10-FQM-6778). Juan J. Ternero-Hidalgo acknowledges the assistance of the Ministry of Economy and Competitiveness of Spain for the award of an FPI Grant (BES-2013-064425).

### References

- [1] C. Moreno-Castilla, M.V. López-Ramón, F. Carrasco-Marín, Changes in surface chemistry of activated carbons by wet oxidation, *Carbon* 38 (2000) 1995–2001.
- [2] J.L. Figueiredo, M.F.R. Pereira, M.M.A. Freitas, J.J.M. Orfao, Modification of the surface chemistry of activated carbons, *Carbon*. 37 (1999) 1379–1389.
- [3] N. Tancredi, T. Cordero, J. Rodríguez-Mirasol, J.J. Rodríguez,  $\text{CO}_2$  gasification of eucalyptus wood chars, *Fuel*. 75 (1996) 1505–1508.
- [4] J.M. Rosas, J. Bedia, J. Rodríguez-Mirasol, T. Cordero, Preparation of hemp-derived activated carbon monoliths. Adsorption of water vapor, *Ind. Eng. Chem. Res.* 47 (2008) 1288–1296.
- [5] J.M. Rosas, J. Bedia, J. Rodríguez-Mirasol, T. Cordero, HEMP-derived activated carbon fibers by chemical activation with phosphoric acid, *Fuel*. 88 (2009) 19–26.

- [6] J.M. Rosas, J. Bedia, J. Rodríguez-Mirasol, T. Cordero, On the preparation and characterization of chars and activated carbons from orange skin, *Fuel Process. Technol.* 91 (2010) 1345–1354.
- [7] M.O. Guerrero-Pérez, M.J. Valero-Romero, S. Hernández, J.M.L. Nieto, J. Rodríguez-Mirasol, T. Cordero, Lignocellulosic-derived mesoporous materials: An answer to manufacturing non-expensive catalysts useful for the biorefinery processes, *Catal. Today.* 195 (2012) 155–161.
- [8] R. Arrigo, M. Hävecker, S. Wrabetz, R. Blume, M. Lerch, J. McGregor, et al., Tuning the acid/base properties of nanocarbons by functionalization via amination, *J. Am. Chem. Soc.* 132 (2010) 9616–9630.
- [9] M. Abe, K. Kawashima, K. Kozawa, H. Sakai, K. Kaneko, Amination of activated carbon and adsorption characteristics of its aminated surface, *Langmuir*, 16 (2000) 5059–5063.
- [10] I. Bautista-Toledo, J. Rivera-Utrilla, M.A. Ferro-García, C. Moreno-Castilla, Influence of the oxygen surface complexes of activated carbons on the adsorption of chromium ions from aqueous solutions: Effect of sodium chloride and humic acid, *Carbon.* 32 (1994) 93–100.
- [11] X. Song, H. Liu, L. Cheng, Y. Qu, Surface modification of coconut-based activated carbon by liquid-phase oxidation and its effects on lead ion adsorption, *Desalination.* 255 (2010) 78–83.
- [12] C. Moreno-Castilla, F. Carrasco-Marín, C. Parejo-Pérez, M.V. López Ramón, Dehydration of methanol to dimethyl ether catalyzed by oxidized activated carbons with varying surface acidic character, *Carbon.* 39 (2001) 869–875.

- [13] J. Bedia, R. Barrionuevo, J. Rodríguez-Mirasol, T. Cordero, Ethanol dehydration to ethylene on acid carbon catalysts, *Appl. Catal. B Environ.* 103 (2011) 302–310.
- [14] J. Bedia, R. Ruiz-Rosas, J. Rodríguez-Mirasol, T. Cordero, Kinetic study of the decomposition of 2-butanol on carbon-based acid catalyst, *AIChE J.* 56 (2010) 1557–1568.
- [15] J. Bedia, J.M. Rosas, J. Rodríguez-Mirasol, T. Cordero, Pd supported on mesoporous activated carbons with high oxidation resistance as catalysts for toluene oxidation, *Appl. Catal. B Environ.* 94 (2010) 8–18.
- [16] W. Kiciński, M. Szala, M. Bystrzejewski, Sulfur-doped porous carbons: Synthesis and applications, *Carbon.* 68 (2014) 1–32.
- [17] M. Calzado, M.J. Valero-Romero, P. Garriga, A. Chica, M.O. Guerrero-Pérez, J. Rodríguez-Mirasol, et al., Lignocellulosic waste-derived basic solids and their catalytic applications for the transformation of biomass waste, (2014).
- [18] S.A.C. Carabineiro, A.M. Ramos, J. Vital, J.M. Loureiro, J.J.M. Órfão, I.M. Fonseca, Adsorption of SO<sub>2</sub> using vanadium and vanadium-copper supported on activated carbon, *Catal. Today.* 78 (2003) 203–210.
- [19] J.M. Rosas, R. Ruiz-Rosas, J. Rodríguez-Mirasol, T. Cordero, Kinetic study of the oxidation resistance of phosphorus-containing activated carbons, *Carbon.* 50 (2012) 1523–1537.
- [20] X. Wu, L.R. Radovic, Inhibition of catalytic oxidation of carbon/carbon composites by phosphorus, *Carbon.* 44 (2006) 141–151.

- [21] A. Elmouwahidi, Z. Zapata-Benabithé, F. Carrasco-Marín, C. Moreno-Castilla, Activated carbons from KOH-activation of argan (*Argania spinosa*) seed shells as supercapacitor electrodes, *Bioresour. Technol.* 111 (2012) 185–190.
- [22] H. Itoi, H. Nishihara, T. Ishii, K. Nueangnoraj, R. Berenguer-Betrián, T. Kyotani, Large pseudocapacitance in quinone-functionalized zeolite-templated carbon, *Bull. Chem. Soc. Jpn.* 87 (2014) 250–257.
- [23] C. Pevida, M.G. Plaza, B. Arias, J. Feroso, F. Rubiera, J.J. Pis, Surface modification of activated carbons for CO<sub>2</sub> capture, *Appl. Surf. Sci.* 254 (2008) 7165–7172.
- [24] M. Sevilla, P. Valle-Vigón, A.B. Fuertes, N-Doped Polypyrrole-Based Porous Carbons for CO<sub>2</sub> Capture, *Adv. Funct. Mater.* 21 (2011) 2781–2787.
- [25] Y. Zhao, X. Liu, K.X. Yao, L. Zhao, Y. Han, Superior capture of CO<sub>2</sub> achieved by introducing extra-framework cations into N-doped microporous carbon, *Chem. Mater.* 24 (2012) 4725–4734.
- [26] W.M.A.W.D. Amirhossein Houshmand, Carbon Dioxide Capture with Amine-Grafted Activated Carbon, *Water Air Amp Soil Pollut.* 223 (2011) 827–835.
- [27] J.P.S. Sousa, M.F.R. Pereira, J.L. Figueiredo, Catalytic oxidation of NO to NO<sub>2</sub> on N-doped activated carbons, *Catal. Today.* 176 (2011) 383–387.
- [28] J.P.S. Sousa, M.F.R. Pereira, J.L. Figueiredo, Modified activated carbon as catalyst for NO oxidation, *Fuel Process. Technol.* 106 (2013) 727–733.

- [29] E. Lorenc-Grabowska, G. Gryglewicz, M.A. Diez, Kinetics and equilibrium study of phenol adsorption on nitrogen-enriched activated carbons, *Fuel*. 114 (2013) 235–243.
- [30] J.R. Pels, F. Kapteijn, J.A. Moulijn, Q. Zhu, K.M. Thomas, Evolution of nitrogen functionalities in carbonaceous materials during pyrolysis, *Carbon*. 33 (1995) 1641–1653.
- [31] T.M. Byrne, X. Gu, P. Hou, F.S. Cannon, N.R. Brown, C. Nieto-Delgado, Quaternary nitrogen activated carbons for removal of perchlorate with electrochemical regeneration, *Carbon*. 73 (2014) 1–12.
- [32] R. Pietrzak, XPS study and physico-chemical properties of nitrogen-enriched microporous activated carbon from high volatile bituminous coal, *Fuel*. 88 (2009) 1871–1877.
- [33] J. Jaramillo, P.M. Álvarez, V. Gómez-Serrano, Oxidation of activated carbon by dry and wet methods surface chemistry and textural modifications, *Fuel Process. Technol.* 91 (2010) 1768–1775.
- [34] P. Chingombe, B. Saha, R.J. Wakeman, Surface modification and characterisation of a coal-based activated carbon, *Carbon*. 43 (2005) 3132–3143.
- [35] P. Vinke, M. van der Eijk, M. Verbree, A.F. Voskamp, H. van Bekkum, Modification of the surfaces of a gas-activated carbon and a chemically activated carbon with nitric acid, hypochlorite, and ammonia, *Carbon*. 32 (1994) 675–686.
- [36] H. Hart, C. M. Hadad, L. Craine and D. J. Hart, *Organic Chemistry: A Short Course*. 13th ed. US: Belmont; 2012.

- [37] W. Yantasee, Y. Lin, G.E. Fryxell, K.L. Alford, B.J. Busche, C.D. Johnson, Selective removal of copper(II) from aqueous solutions using fine-grained activated carbon functionalized with amine, *Ind. Eng. Chem. Res.* 43 (2004) 2759–2764.
- [38] S. Tanada, N. Kawasaki, T. Nakamura, M. Araki, M. Isomura, Removal of formaldehyde by activated carbons containing amino groups, *J. Colloid Interface Sci.* 214 (1999) 106–108.
- [39] J. Rodríguez-Mirasol, T. Cordero, J.J. Rodríguez, CO<sub>2</sub>-reactivity of eucalyptus kraft lignin chars, *Carbon.* 31 (1993) 53–61.
- [40] J. Rodríguez-Mirasol, T. Cordero, J.J. Rodríguez, Activated carbons from CO<sub>2</sub> partial gasification of eucalyptus kraft lignin, *Energy Fuels.* 7 (1993) 133–138.
- [41] J. Rodríguez-Mirasol, T. Cordero, J.J. Rodríguez, Preparation and characterization of activated carbons from eucalyptus kraft lignin, *Carbon.* 31 (1993) 87–95.
- [42] D.H. Pote, T.C. Daniel. In: G.M. Pierzynski, editor. *Methods of phosphorus analysis for soils, sediments, residuals, and waters.* North Carolina State University, Publisher; (2000) 94-97.
- [43] C. Moreno-Castilla, M.A. Ferro-García, J.P. Joly, I. Bautista-Toledo, F. Carrasco-Marín, J. Rivera-Utrilla, Activated carbon surface modifications by nitric acid, hydrogen peroxide, and ammonium peroxydisulfate treatments, *Langmuir.* 11 (1995) 4386–4392.
- [44] A.-N.A. El-Hendawy, Influence of HNO<sub>3</sub> oxidation on the structure and adsorptive properties of corncob-based activated carbon, *Carbon.* 41 (2003) 713–722.